Atmospheric Research 255 (2021) 105521

Contents lists available at ScienceDirect

Atmospheric Research

journal homepage: www.elsevier.com/locate/atmosres

Climatology and ranking of hazardous precipitation events in the western Mediterranean area

Damián Insua-Costa [a,b,*], Marc Lemus-Cánovas [c], Gonzalo Miguez-Macho [a,b], María Carmen Llasat [d]

[a] CRETUS Institute, Universidade de Santiago de Compostela, Galicia, Spain
[b] Non-Linear Physics Group, Universidade de Santiago de Compostela, Galicia, Spain
[c] Climatology Group, Department of Geography, Universitat de Barcelona, Catalonia, Spain
[d] GAMA, Department of Applied Physics, Universitat de Barcelona, Catalonia, Spain

ARTICLE INFO

Keywords:
Hazardous rainfall
Mediterranean
Floods
Events ranking
Weather types

ABSTRACT

The western Mediterranean region often suffers from the devastating effects of flooding, caused by enormous rain accumulations that sometimes resemble the values produced by tropical systems. Despite the climatic and social relevancy of this type of episodes, there are some fundamental questions that would still be difficult to answer today, for example: where within the region are more cases recorded? or, which were the most potentially dangerous episodes? In this study, we identify, and then gather and unify information from, all the daily events occurred from 1980 to 2015. Using the MESCAN high-resolution gridded rainfall dataset, events are detected and for each case, the date and affected regions are recorded. Subsequently, events are ranked according to their magnitude and classified by weather type. In addition, flood data from the FLOODHYMEX and EM-DAT databases are used to check whether the precipitation episodes resulted in flooding. All this information is collected into a publicly available single database. Results show that the highest number of events per year is recorded in the Languedoc-Roussillon region (France) and in the Valencian Community (Spain). The cases of greatest magnitude, which are associated with a larger number of floods, present a very marked seasonality, with about 80% of them occurring in September, October and November. Finally, we show that only four weather types are present in most of the days with hazardous rainfall in the western Mediterranean. The most hazardous situation is characterized by a low-pressure area at all tropospheric levels in the eastern Atlantic, forming a block pattern with an anticyclonic ridge that tends to extend from the Central Mediterranean to Central Europe. About 40% of the most extraordinary cases are associated with this configuration. As an example, the infamous Piedmont (Italy) 1994 episode, in the top 10 of the ranking, was produced by an atmospheric pattern of this type.

1. Introduction

High inter-annual or intra-annual variability in the precipitation regime is a recurrent climate feature of much of the most populated regions of our planet. This high variability is directly connected with the incidence of extreme hydro-meteorological events, such as torrential rainfall or droughts (Easterling et al., 2000) and consequently, flood damages or water shortages are issues to which most countries are subject. More specifically, floods, mainly caused by heavy rain (Adhikari et al., 2010), impact more people than any other type of natural hazard in the world, and for this reason, extreme precipitation resulting in inundation has been thoroughly studied with the main objective of reducing the high economic and human costs caused by this type of catastrophic episodes. However, prospects for the future in this respect are not encouraging; studies suggest that global warming is leading toward a more humid atmosphere, increasing the odds of extreme precipitation events (e.g Min et al., 2011; Donat et al., 2016), which could result in higher costs.

The western Mediterranean region (WMR) frequently suffers from the adverse effects of floods, associated with the development of strong convective situations giving rise to relatively short but intense periods of rain. Much of the annual rainfall in the Mediterranean is often accumulated during these heavy precipitation events. Extreme rainfall and flooding are not only essential elements of climate in the WMR, but also

* Corresponding authror.
E-mail address: damian.insua@usc.es (D. Insua-Costa).

https://doi.org/10.1016/j.atmosres.2021.105521
Received 19 May 2020; Received in revised form 10 November 2020; Accepted 11 February 2021
Available online 23 February 2021

key social features due to the enormous impact they cause (Llasat et al., 2010, 2013b; Gaume et al., 2016). Flood episodes such as the case of Tous (Spain) in October 1982 or Piedmont (Italy) in November 1994 have been analysed by researchers (e.g. Romero et al., 2000; Buzzi et al., 1998) and are still remembered by the population and the media because they claimed the lives of more than 100 people (Barredo, 2007). Moreover, studies show that, in some parts of this region, heavy daily rainfall and flooding occurrence have increased in recent years (Alpert et al., 2002; Diakakis, 2014; Llasat et al., 2013b, 2016) and will continue to do so in the coming decades (e.g. Sánchez et al., 2004; Gao et al., 2006; Goubanova and Li, 2007; Tramblay and Somot, 2018) coinciding with the expected trend in the global precipitation regime to become more extreme. Therefore, prevention and research in the field of extreme rains and floods in the Mediterranean must continue to advance in bringing together efforts from different countries and disciplines, as it is currently the case within the HYMEX international program (Drobinski et al., 2014; Ducrocq et al., 2014).

In spite of all the aforementioned research efforts, there are, however, some apparently simple but very important questions that have so far not yet been answered, such as: where do more potentially catastrophic precipitation events occur? How many events are registered annually? Or, which ones were the most hazardous? The main objective of this work is to obtain a comprehensive characterization of all precipitation events that had the potential to cause significant damage occurred throughout the entire WMR from 1980 to 2015, thereby providing answer, among others, to the questions posed above.

Detecting the potentially catastrophic precipitation episodes that have affected the WMR would require a very high density of precipitation data, given their very high spatial variability. However, rain gauges are often too far apart from each other and even where the rain gauge density is sufficient, the data is frequently not open access; therefore, the task is hampered by the unavailability of observations in many areas within the region. Early studies in the United States evidenced the same observational constraint. Brooks and Stensrud (2000) presented a climatology of heavy rains on short timescales and, in spite of the high station density used, found that their results presented important deficiencies since many of the events were not correctly detected by the observational network.

In the WMR, however, the studies conducted on extreme and heavy precipitation are solely based on rain gauge data. Romero et al. (1998) built a daily heavy rainfall database from 1964 to 1993 in the Spanish Mediterranean Regions using data from 410 weather stations. They considered as extreme those days in which daily rainfall exceeded 100 mm and confirmed that many of the events took place in the surroundings of the Sierra de Aitana (Alicante) during autumn. More recently, Ramos et al. (2014) created a ranking of extreme daily precipitation events in the Iberian Peninsula, including the Spanish Mediterranean area. They used the IB02 precipitation database (Belo-Pereira et al., 2011; Herrera et al., 2012), derived from data collected by more than 2800 rain gauges spread throughout Iberia. Using a pluviometric threshold based on normalized precipitation anomalies, they found, for example, that the major episode affecting this region between 1950 and 2008 was that of November 1982. In Italy, Brunetti et al. (2002) employed precipitation data from 75 observation stations and detected a total of 87 extreme precipitation events in the period 1951–2001. For the definition of extreme event, they considered a threshold based on the average annual precipitation recorded by each station. In France, Ricard et al. (2012) elaborated a heavy precipitation event database using more than 1200 rain gauges located in the southern part of the country. They worked with a constant threshold of 150 mm for identifying days with extreme rainfall and found 305 episodes in the period 1967–2006. Jansa et al. (2001), in the context of the MEDEX project (Jansa et al., 2014), analysed a wider region, covering much of the WMR from 1991 to 1996. In this case they applied a threshold of 60 mm/24 h for the whole region, except in Algeria where the threshold was of 30 mm/24 h.

In summary, all the aforementioned earlier studies provide valuable information but are limited by the exclusive use of in situ precipitation measurements. Furthermore, they all analyse different sub-regions within the WMR and the methods employed to detect heavy or extreme precipitation episodes vary widely from study to study, which evidences that defining extreme or heavy event is a controversial point, since each researcher usually imposes one criterium of his or her own. In addition, these studies use precipitation thresholds that are not necessarily related to impacts; thus, they cannot provide a general analysis within the WMR of events with the potential to cause damage.

Indeed, whether or not introducing impacts into the definition of extreme events is a hotly debated topic today (e.g. McPhillips et al., 2018). In the literature, extreme precipitation generally refers to precipitation that exceeds a statistical threshold, for example a percentile, and the term heavy precipitation is usually reserved for rainfall that exceeds a constant threshold, for example 100 mm. However, neither extreme nor heavy precipitation are necessarily extreme in terms of impacts (Seneviratne et al., 2012); thus, a specific strategy is required to identify hazardous events. To avoid confusion, from now on we will use the terms “extreme” or “heavy” in the conventional scientific sense, avoiding colloquial interpretations, and we will use the terms “hazardous” or potentially catastrophic precipitation for those amounts of rain that have the potential to produce important damages. Therefore, hazardous precipitation events (HPEs) are the focus of our study.

Although defining a threshold associated with impacts can be tremendously complex, a very recent study (Liu et al., 2020) shows that the combination of a fixed precipitation threshold with a statistical one (in their case, a percentile) provides the highest correlation with economic losses, and we will use a similar strategy to identify the events to consider in our case. Additionally, we will use flood databases to verify that the selected events were indeed mostly conducive to damages.

Our precise goals are to obtain a detailed picture of the spatial and temporal distribution of HPEs in the Western Mediterranean, a ranking of events according to their magnitude and a classification by weather type assigning a characteristic atmospheric pattern to each. Our analysis of the atmospheric conditions that usually generate hazardous rainfall situations in the WMR will be more concise and have a more general scope than in previous studies, which most often only focus on a small part of the region, obtaining a large number of potential patterns (e.g. Romero et al., 1999; Lana et al., 2007; Federico et al., 2008; Houssos et al., 2008; Martínez et al., 2008; Gilabert and Llasat, 2018) that make it difficult to establish a simple and clear overview of the synoptic configurations that affect the region as a whole.

All the resulting information from our study will be compressed in a single database. Thus, the main novelties of such database, and in general of this research, are: (1) it includes events from the entire WMR and for a long period (36 years), (2) the information it provides goes beyond the spatiotemporal location of the episodes, since it also contains additional data such as the magnitude or the associated weather type, (3) it is based on a gridded high-resolution precipitation dataset, built not only from rain gauge measurements and, therefore, avoiding in part the observational deficiency that affects other studies and (4) the events in the database are detected using an impact related threshold. The generated HPE database will be freely accessible to other authors.

The study is structured as follows: Section 2 and 3 describes, respectively, the data and the methodology used. In these sections we show, for example, the high-resolution precipitation database used and the selected method to detect the events. Section 4 discusses results, where we present the HPE database and the climatology created. Finally, Section 5 contains a summary and conclusions of the work.

2. Data

2.1. Precipitation datasets

For the detection of HPEs, we use the MESCAN precipitation analysis system (Soci et al., 2016), which has been recently developed within the

European Reanalysis and Observations for Monitoring (EURO4M) project (http://www.euro4m.eu). It comes from the merger of two previous surface analyses (hence its name): MESan (Häggmark et al., 2000) and (Taillefer, 2002). MESCAN is based on a model background field adjusted with observations. The background data is a reanalysis generated from the HIRLAM model and downscaled from 22 to 5.5 km. Rain gauge measurements are from a high-density observational network covering the whole of Europe. Thus, it provides accurate daily gridded rainfall data from 1961 to 2015, which are especially useful for climatological purposes.

The two main advantages of MESCAN are: (1) it includes our entire region (the WMR) and period (1980–2015) of interest, so we do not have to mix data from different precipitation datasets, often incompatible because of their dissimilar characteristics and (2) by using a high-resolution reanalysis as background field, it provides a good precipitation estimate compared with other methods that only use rain gauge data, especially in places where there are no direct measurements. Therefore, it is very appropriate for capturing heavy precipitation events. Its main drawbacks are: (1) its temporal resolution is only one day, so it is not suitable for detecting very short duration events and (2) assimilated rain gauge observations are inhomogeneously distributed, which could result in diminished event detection numbers in some parts of the region, not because of climatological factors but because of a lower observational density.

In order to evaluate the impact of deficiency (2) above on detection skill, we compare the results obtained from MESCAN with those from two other precipitation databases, the SPREAD (Serrano-Notivoli et al., 2017) and the APGD (Isotta et al., 2014) gridded datasets, both constructed using a very dense observational network and at the same spatial resolution of 5 km, which is similar to that of MESCAN (5.5 km), thus making them especially appropriated for the validation of the latter. SPREAD covers Spain and APGD the entire Alpine region, areas where the observational density of MESCAN is lower than, for example, in France. Results show (see Fig. S1 in the Supplementary Material) that despite the reduced number of ingested observations in MESCAN in these areas, HPEs are still well captured, since the number of detections is in good agreement with that obtained with SPREAD and APGD. Therefore, we conclude that this drawback does not significantly affect the results obtained in this study.

Fig. 1a shows the average annual precipitation over Europe and northern Africa from MESCAN. Its high resolution (5.5 km) is very evident in how it adequately reproduces the strong orographic dependence of precipitation. Fig. 1b shows the same field but from E-OBS v20.0e (Cornes et al., 2018), one of the most widely used gridded precipitation datasets. Although both are generally similar in terms of magnitude, the spatial distribution of precipitation in E-OBS is less realistic than in MESCAN. For example, E-OBS is not able to properly represent the orographic enhancement of precipitation in the different mountain systems of the region, a deficiency mainly due to the exclusive use of interpolated observations to build the gridded database. In summary, we argue that, for our purpose, MESCAN is much more suitable than other datasets.

2.2. Flooding data

We use flooding occurrence data from the FLOODHYMEX (Llasat et al., 2013b,a) and EM-DAT (http://www.emdat.be/) datasets to further characterize the detected events in our HPEs database. Additionally, we employ flooding information in these datasets to validate our HPEs detections. As floods (including urban floods, flash-floods and surface water floods) in the Mediterranean region are mainly rainfall-related, flood data can be crossed with HPEs identified from MESCAN precipitation data to ensure that detections are indeed correct.

The FLOODHYMEX database was developed in the framework of the HYMEX project, hence its name. It contains information about the date, place, physical features of the hazard (precipitation, discharge, etc) and impacts of all the catastrophic or large floods recorded in a selected region of the Mediterranean for a given period. They are identified as catastrophic in basis of the methodology usually applied to classify flood events according to their impact (Barriendos et al., 2003; Llasat et al., 2016); that is, it provides information about integrated flood risk, not flood hazard (as it would be the case if using discharge data alone). FLOODHYMEX was created with the ambition of becoming a common database of damage producing floods in the Mediterranean region, based on a rigorous analysis of daily information and using the same criteria to characterise all the events and regions (Llasat et al., 2013a). FLOODHYMEX includes floods in Spain (Catalonia, Valencian Community and the Balearic Islands), France (Languedoc-Roussillon, Midi-Pyrenees, Provence-Alpes-Côte d'Azur), Italy (Calabria) and Greece. The database currently covers the 35-year period from 1981 to 2015. In total, FLOODHYMEX contains information on 171 flood events, which can have a duration of one or more days and affect one or several

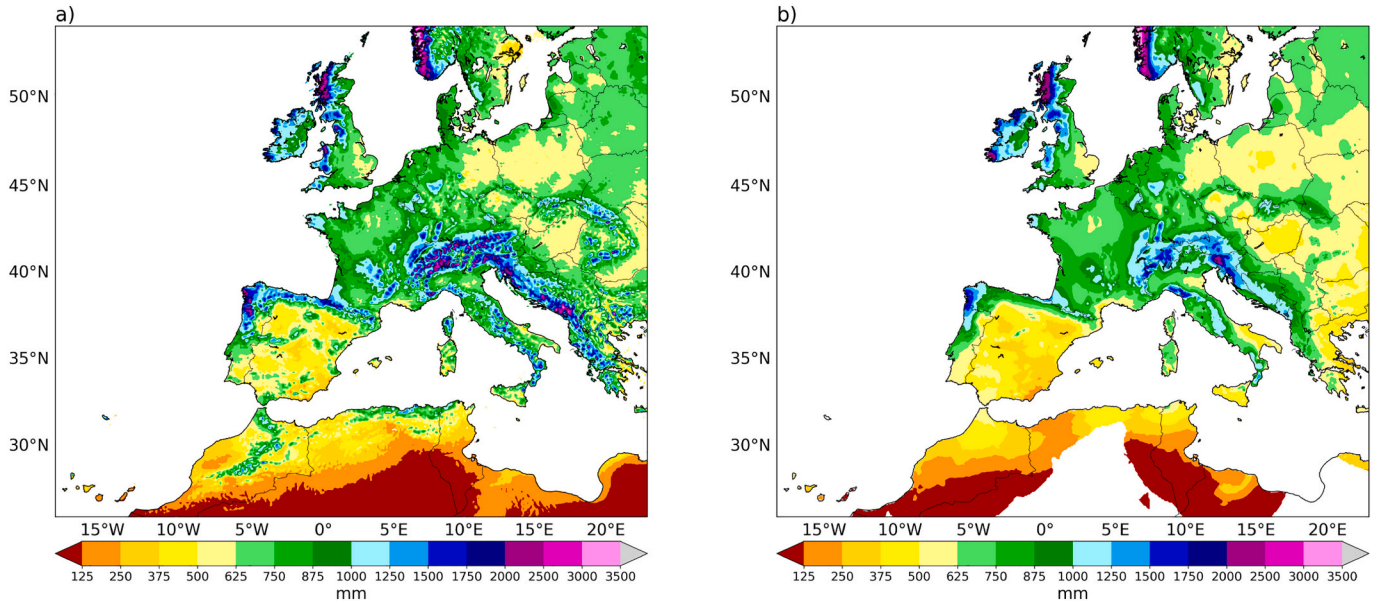

Fig. 1. Annual mean precipitation on land from MESCAN (a) and form E-OBS (b) for the climatological period 1980–2015.

regions. The latest public version can be found at http://mistrals.sedoo.fr/?editDatsId=1150datsId=1150project_name=MISTRALSq=floodhymex.

The main advantage of FLOODHYMEX is the highly detailed information it provides. Its main disadvantage is that it does not fully cover our region of interest and study period. For this reason, we use an additional flood dataset, EM-DAT (Emergency Events Database), which employs more restrictive criteria than FLOODHYMEX, thereby including less cases, but it is global, so it covers the whole Mediterranean region and for a long period (from 1900 onwards). FLOODHYMEX will be our reference flood database, but in areas or periods not covered by it, the information will be completed with EM-DAT.

2.3. ERA5 reanalysis

ERA5 (Hersbach and Dee, 2016) is the most recent (5th generation) global atmospheric reanalysis of the European Centre for Medium-Range Weather Forecasts (ECMWF), providing hourly data from 1979 to near-real time. ERA5 stands out for its high resolution (31 km in horizontal and 137 vertical levels), as well as for the vast amount of historical assimilated observations, and it represents a major improvement over its predecessor, the ERA-Interim reanalysis. We use ERA5 to classify HPEs according to the associated weather types. The variables used here for such classification are geopotential at 500 hPa, sea level pressure and precipitation, which have been obtained for the entire study period (1980–2015) every 6 h.

3. Methodology

3.1. Region of study

The selected region of study is shown in Fig. 2, in which each coloured area indicates a different sub-region. We have considered the zones of Spain, France and Italy surrounding the western sector of the Mediterranean Basin. Hereafter, the term WMR refers to the combination of these regions. We note that the African part of the Mediterranean region is not considered in this study.

To select the region of study we use the Nomenclature of Territorial Units for Statistics or NUTS (by its French acronym), a standard for the classification of the territory used by the European Union. This standard subdivides the EU Member States into three categories (NUTS1, NUTS2 and NUTS3) according to socio-economic criteria. The reason for using this method is that it will make simpler to cross our HPEs dataset with others, since many of them are built using the same territorial classification, such as the FLOODHYMEX database. Table S1 in the Supplementary Material shows for each region the names of the different NUTS encompassed, along with additional information, such as total area. Note that Andorra is not included in the table because it is not a EU Member State, but it is part of Region 2.

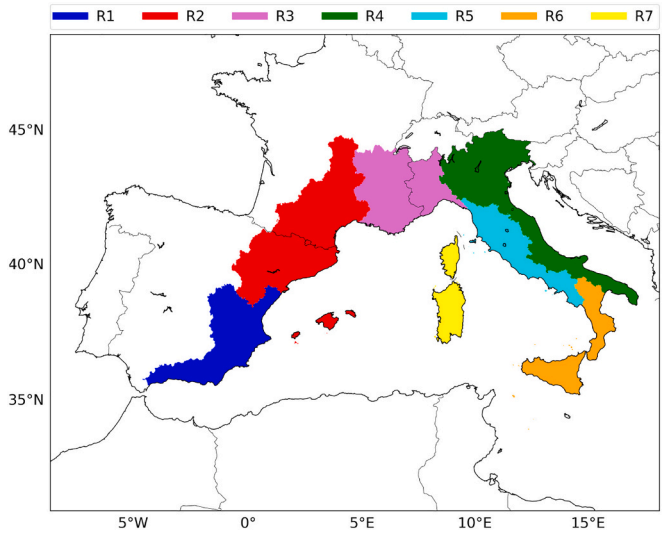

Fig. 2. Region of study. Each colour represents a different sub-region.

The grouping of these territories into different sub-regions is based on a climatological criterion relying on our previous experience, the distribution of the relief and large scale atmospheric flow exposure. For example, some areas within Region 1 will generally be affected by heavy rainfall when the wind is from the east, while Region 2 will be more favoured by south-easterly flows and Region 3 by southerly winds (see fourth column in Table S1). The selection of a climatological instead of a political criterion explains why some regions are formed by territories from different countries.

In Fig. 3 we show two important characteristics of the region. First, its abrupt orography (Fig. 3b) with multiple mountain systems, among which the Pyrenees (Region 2) and the Alps (Region 3 and 4) stand out. All the sub-regions present a pronouncedly rough terrain, with elevations from sea level to mountains well above 2000 m. And second, its average precipitation (Fig. 3a), which is strongly linked to the topography, with the highest values (more than 2000 mm per year) being found in the highest mountains of the Alps and Apennines (Region 3 and 4). The Spanish sector is clearly the driest, mainly Region 1, where annual rainfall is below 400 mm over a large area.

3.2. Setting a threshold for hazardous day detection

In this work the threshold is based on normalized daily precipitation anomalies, a method recently used by Ramos et al. (2014) to detect and rank extreme precipitation events in the Iberian Peninsula. For a given MESCAN grid point (i, j), the normalized departure from the climatology (N_{ij}) of a daily precipitation amount P_{ij} is:

$$N_{ij} = \frac{P_{ij} - \overline{P_{ij}}}{\sigma_{ij}} \quad (1)$$

where $\overline{P_{ij}}$ is the mean daily precipitation and σ_{ij} is the standard deviation (std) from this daily mean. We introduce three novelties with regard to the methodology used by Ramos et al. (2014, 1) we don't use a running mean to calculate the mean daily precipitation and std., (2) we consider all days in the calculation of the daily mean and std., not only wet days and (3) we impose a minimum value in the threshold. The main reason to avoid a running mean is that we wanted a static threshold that could be applied indistinctly to every day of the year. In addition, we take into account dry days in the calculations because it is essential to properly characterize the precipitation variability and because some previous studies have shown that the widely used approach of discarding dry days (e.g. Schär et al., 2016) can sometimes lead to misleading results.

Including dry days, results in our daily mean and std. taking lower values, and for this reason, we detect a daily precipitation event when at least in one MESCAN grid cell the precipitation anomaly reaches ten standard deviations, i.e., $N_{ij} > 10$, instead of the $N_{ij} > 2$ used in Ramos et al. (2014). Therefore, if we keep in mind Eq. (1), our threshold (T_{ij}) could be written as:

$$T_{ij} = \overline{P_{ij}} + 10\sigma_{ij} \quad (2)$$

and the condition to detect an event in a grid point (i, j) will be $P_{ij} > T_{ij}$. Since daily means tend to be small (especially when considering also dry days), the previous equation is dominated by $\sqrt{\sum {P_{ij}}^2}$; therefore, the wettest places, and especially those with frequent large daily precipitation records, will have a more demanding threshold, which makes sense because they are likely the best adapted to high precipitation amounts.

Nevertheless, this statistical threshold can take too low values in some places of our region, of around 30 mm, especially in semi-desert

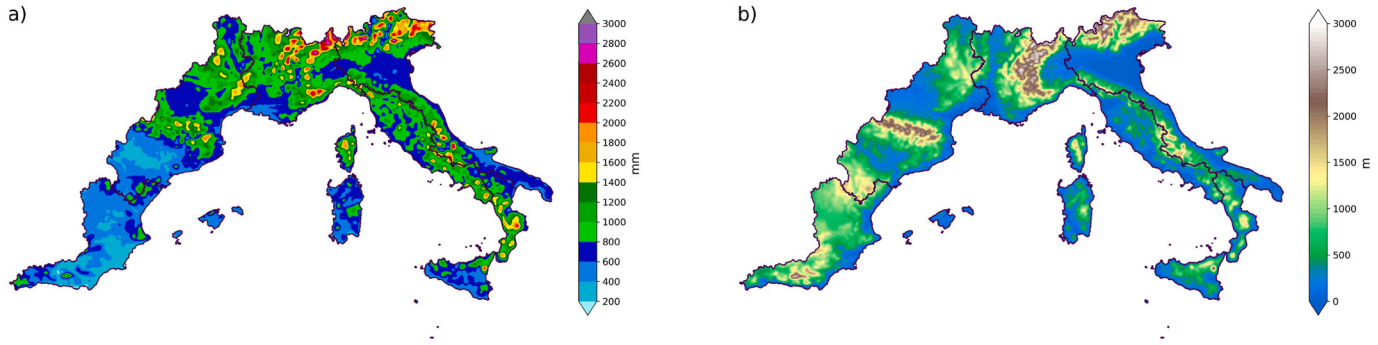

Fig. 3. Annual mean precipitation for the climatological period 1980–2015 (a) and topography (b) of the western Mediterranean region.

areas of Spain. From the perspective of impacts, a relatively small rain amount could cause damage, for example, due to the presence of a soil with low infiltration capacity; however, in the WMR, large rainfall accumulations are usually needed to wreak havoc. Thus, we impose a minimum value in the threshold, which we set at 60 mm according to the criteria used in the MEDEX project (Jansa et al., 2014). Since we are working with a gridded rainfall database, the threshold is applied at each grid cell, i.e. to the value representing the spatially averaged rainfall in a region of $5.5km^2$ (the resolution of MESCAN), thus a value of 60 mm certainly translates into higher local (sub-grid) values.

In summary, in this study we use a combination of a statistical precipitation threshold with a fixed one, given that the minimum value can also be regarded as a constant threshold. This is the same approach used in Liu et al. (2020) to set an impact-related threshold. Fig. 4 shows the combined threshold, which we ultimately use for the detection of potentially catastrophic precipitation events. It ranges from 60 mm, i.e. the minimum value, to more than 140 mm in some mountainous areas., which indicates that our threshold adapts to the climatic characteristic of each location. For example, in the Alps, daily rainfall of about 100 mm is relatively frequent due to the orographic enhancement of precipitation; thus, the threshold is more demanding there, so that only days with higher than normal rainfall are considered. The number of days in which this threshold is exceeded in at least one point in the region's grid across the 36-year period analysed is 1991.

3.3. Classifying hazardous days by weather type

In this study the methodology used to classify HPEs by weather types is based on a principal component analysis (PCA) approach, a widely used methodology to this end (Esteban et al., 2005; Philipp et al., 2016; Lemus-Canovas et al., 2019c; Lemus-Canovas et al., 2019b). We apply a PCA to a temporal mode (T-mode) matrix of 500 hPa geopotential height, mean sea level pressure and daily precipitation, all of them obtained from ERA5 reanalysis data for consistency. Thus, in the T-mode matrix, the variables (columns) are the 1991 hazardous days identified, and the observation (rows) are the grid points from the ERA5 geographical area used (30°-50°N, 15°W-23°E). For a given HPE, the values of sea level pressure and 500 hPa geopotential are taken at the time of maximum precipitation of the day, which is determined from 6-hourly ERA5 precipitation, so that if the maximum rainfall is recorded from 18 to 00 UTC, the considered fields correspond to 18 UTC. This strategy responds to the rapidly evolving nature of many of the weather systems resulting in HPEs, whereby daily means of the meteorological variables may not represent properly the conditions leading to the observed high rainfall accumulations.

After applying the PCA to the previously standardized original data matrix, new variables are obtained, the principal components (PC), which are linear combinations of the original variables. The method employed to determine the number of components to retain is the well-known Scree Test (Cattell, 1966), based on the amount of explained variance by each PC. These PCs are subsequently rotated by means of a varimax rotation, in order to obtain the maximum variance explained for each PC (Richman, 1986). From the rotated PCs we obtained the loadings, the correlation matrix, which indicates the degree of correlation of all considered days with each PC. In this sense, the assignment of each day to each PC is based on the maximum correlation value. Day 1 is assigned to the PC with the highest correlation, and so on. This methodology allows classing each of the events into a unique weather type, even when their correlation with all PCs is low. To account for this lack of representativeness in some cases, the days whose correlation with all PCs is <0.4, are assigned as undefined. The R package synoptReg (Lemus-Canovas et al., 2019a) is used to develop such classification.

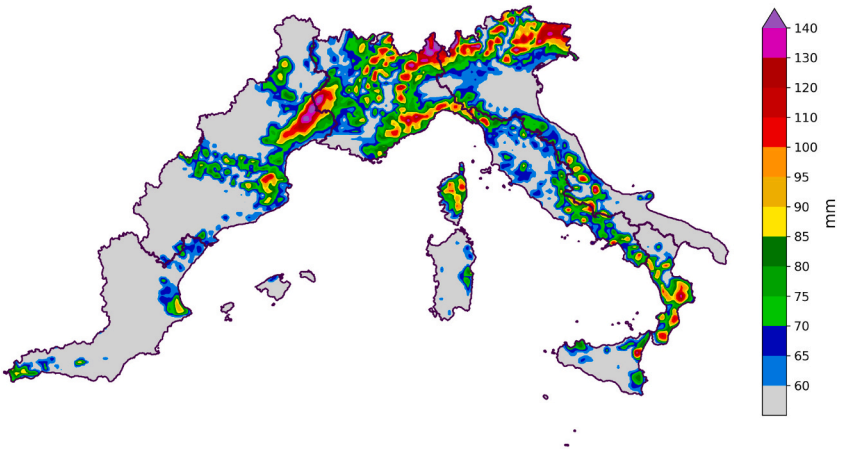

Fig. 4. Threshold (mm) used to detect potentially catastrophic daily rainfall. Grey indicates 60 mm.

After applying this method, each day with potentially catastrophic rainfall will be associated with a (single) weather type.

3.4. Ranking events by magnitude

Once all the daily events in our period of interest have been identified, we order them according to their magnitude, obtaining a ranking in which the events at the top are the most hazardous, potentially causing high damage. Following the recommendations of the World Meteorological Organization, the magnitude in a grid point i,j will be defined as the difference between the accumulated rainfall (P_{ij}) and the established threshold for that point (T_{ij}):

$$m_{ij} = P_{ij} - T_{ij} \tag{3}$$

and the overall magnitude of the event will be:

$$M = \overline{m}A \tag{4}$$

where $\overline{m}$ is the spatial average of the local magnitudes and A is the fraction of the total continental area of the WMR affected by the episode, i.e. the area where the threshold (Fig. 4) is exceeded. In summary, for an event to be of high magnitude, it must affect a large region or, if not, very intensely affect a smaller region. If the event produces highly above-threshold precipitation over a large region, an extraordinary magnitude is assured.

4. Results

4.1. Spatial distribution of hazardous rains

For each MESCAN grid cell, the number of days on which the corresponding threshold (Fig. 4) is exceeded during the period 1980–2015, i.e., the total number of days with hazardous rainfall, is shown in Fig. 5.

An important conclusion can be drawn immediately from Fig. 5: HPEs are concentrated in only a small part of the WMR, organized in coastal strips with two main extensions inland. The coastline from Murcia (Spain) to Genoa (Italy) across Regions 1, 2 and 3, is the most affected. The other coastal stretches impacted are the Ionian coasts of Calabria and Sicily (Region 6) and the Tyrrhenian coasts of the islands of Corsica and Sardinia (Region 7). In France hazardous rainfall extends inland along the south eastern sector of the French Massif Central as well as up the Rhone Valley. For its part, in Italy, the potentially catastrophic precipitation is extended towards the western Alps from the heavily impacted shores of Liguria. We note that the largest number of episodes are not recorded in the highest zones. In the Alps, the most affected area is the mountain slope rising west from the Po Valley. This does not mean that in these high elevation locations rainfall has to be necessarily less, but that the same rain accumulation might not be statistically extreme there. In any case, the orography plays a major role, since it is fundamental in producing precipitation enhancement in the high mountains, but also in lower areas at their foot. In addition, there are also other small affected zones spread irregularly throughout the region, such as the coast around Malaga (Spain, Region 1) or Naples (Italy, Region 5).

Among regions as a whole, 1, 2 and 3 are the most affected, whereas 4 and 5 are the least. The areas surrounding the Gulf of Lion (Region 2) and the coastal strip of the Valencian Community (Region 1) are the most exposed to hazardous rains in the entire region. Here we find the absolute maximum value of potentially catastrophic rain days, with around 30 from 1980 to 2015, almost one per year. The rest of the frequently affected territories, including the Liguria and Piedmont regions or the east coast of Corsica, Sardinia, Calabria and Sicily, have similar values, greater than 15 days over a vast area, with peaks of more than 20 days especially in region 6.

From Fig. 5 we can also infer that within the WMR the main factor for the occurrence of hazardous rains is the proximity to the coast. This is a key point in relation to flood risk, because most of the region's population is settled in coastal areas. Some of the region's major cities are thus heavily exposed to torrential rains. The southern or eastern orientation of the coastline also appears to be a crucial factor, suggesting that southerly or easterly flows at low levels are often associated with stronger thermal or dynamic instability situations. In the WMR, warm and moist air advection is almost assured when the wind blows from these directions, which favours the accumulation of large amounts of rain. This is why the Western Mediterranean Oscillation (WeMO; Martin-Vide and Lopez-Bustins, 2006) is a good predictor of heavy rainfall in this area (Lopez-Bustins and Lemus-Canovas, 2020), since its negative phase is univocally associated with these southerly or easterly wind components (Martin-Vide et al., 2008). As stated above, orography also plays a very important role. As evidence, note that maximum values in Fig. 5 generally appear as peaks located very close to the sea, but slightly inland, which means that small slopes near the most affected coastal stretches can substantially enhance heavy rainfall.

Finally, we note that, since we are working with daily rainfall data, this climatology does not include most very short duration episodes, such as a case of 30 mm in 1 h associated with strong afternoon convection. These brief episodes, although may cause some local damage, are not usually associated with major disasters. There are, however, some cases, where a local storm discharges vast amounts of water onto a very vulnerable site, potentially causing devastating flash floods. Inevitably, such episodes will not be adequately captured by MESCAN because of their local nature. In addition, since they affect very small areas, their magnitude cannot be classified as exceptional in terms of

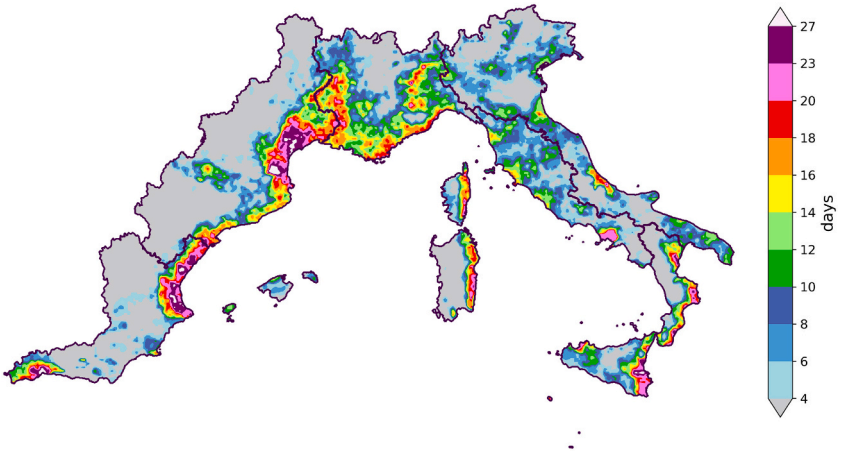

Fig. 5. Spatial distribution of hazardous precipitation in the western Mediterranean region: total number of potentially catastrophic rain days from 1980 to 2015. Grey indicates 0 to 3 days.

generated rainfall from the broader perspective of the entire Western Mediterranean region. They can, nevertheless, be exceptional from the point of view of impacts, but these are subject to other factors that have nothing to do with precipitation. Had we considered these episodes of very reduced temporal and spatial scale, the values shown in Fig. 5 would have increased substantially.

4.2. Magnitude of events

Here we group events according to their magnitude in bins of 25 and calculate within each bin the fraction of cases that appear also in FLOODHYMEX and/or EM-DAT. Results are depicted in Fig. 6. If the assignment of magnitude were correct, the more hazardous the events in the bin are, the greater the number of flood occurrences. Fig. 6 shows that more than 80% of the most hazardous cases (bin 1) are associated with flooding and that in general this percentage is reduced by lowering the magnitude, which suggests that the used method works. Note that the used flooding datasets generally contain only severe floods, so these percentages could be higher if we had also considered minor flooding episodes. Table 1 shows these 25 extraordinary cases ranked by magnitude. The specific numerical values obtained by applying Eq. (4) are not shown because they lack physical sense; they are only used to order the events. 21 out of the 25 episodes led to flooding, which is an indication of their severity, and indeed most of the events in this table are easily recognizable by the impact they caused. Some examples are the catastrophic floods produced in the Gard event of September 2002 (in 9th position; Milelli et al., 2006) or in the more recent Genoa event of November 2011 (in 5th position Fiori et al., 2014). A particularly remarkable case is that of November 1982, first in our ranking, which caused devasting floods in Andorra, Spain and France (Trapero et al., 2013), as Ramos et al. (2014), using other data and methods, also found this event to be the most extreme since at least 1950 in the Iberian Peninsula. This demonstrates its exceptionality in climatological terms.

In some cases, a bin of events of lesser magnitude may be associated with a greater number of floods. It should always be borne in mind that flooding and its effects do not only depend on the meteorological variables, but are also subject to other factors, such as land use or population density, which could increase vulnerability, thus risk. Care should also be taken in interpreting the position of events in the ranking. The magnitude of the events is obviously subject to an uncertainty derived from the possible inaccuracies in the amounts of rainfall provided by MESCAN.

Table 1
The first 25 episodes in the HPEs database, i.e., the 25 episodes with the highest magnitude (those in the first bin of Fig. 6). For each episode (rows) we show in columns (from left to right): the position in the ranking, dates, the affected regions, the associated weather type and whether or not there was flooding, according to FLOODHYMEX and EM-DAT data.

Number ranking	Date	Regions	Weather type	Floods
1	1982-11-07	R1-R2-R3	1	YES
2	1999-11-12	R2-R7	3	YES
3	2003-12-01	R2-R3	1	YES
4	1993-09-23	R2-R3-R4-R5-R7	2	YES
5	2011-11-05	R2-R3-R6-R7	1	YES
6	1994-11-05	R3-R4-R5-R7	1	YES
7	2000-10-23	R1-R2	3	YES
8	1993-09-22	R2-R3	2	YES
9	2002-09-08	R2-R3	1	YES
10	1992-09-26	R1-R2	1	YES
11	1987-11-04	R1	3	YES
12	1989-09-04	R1-R2	3	YES
13	1982-02-16	R2	3	YES
14	1994-01-06	R2-R3	1	NO
15	2000-10-14	R3-R5-R7	U	YES
16	2014-11-04	R3-R4	2	YES
17	2010-06-15	R3	2	YES
18	2006-01-30	R2-R6-R7	U	NO
19	1996-11-12	R2-R3	3	NO
20	1982-10-20	R1	3	YES
21	2010-10-10	R2-R6-R7	3	YES
22	2003-12-03	R2	3	YES
23	1997-09-30	R1	3	YES
24	2009-09-28	R1	3	NO
25	1996-09-11	R1-R2	3	YES

4.3. Weather types causing potentially catastrophic precipitation

We classify all identified events into four groups according to the maximum correlation with one of the four principal components considered and then we obtain average maps for each of these groups of days. Fig. 7 shows these average maps, which represent the most recurrent atmospheric patterns in the WMR when potentially catastrophic rainfall occurs, as combined they explain 77% of the total variance. A greater number of principal components would have

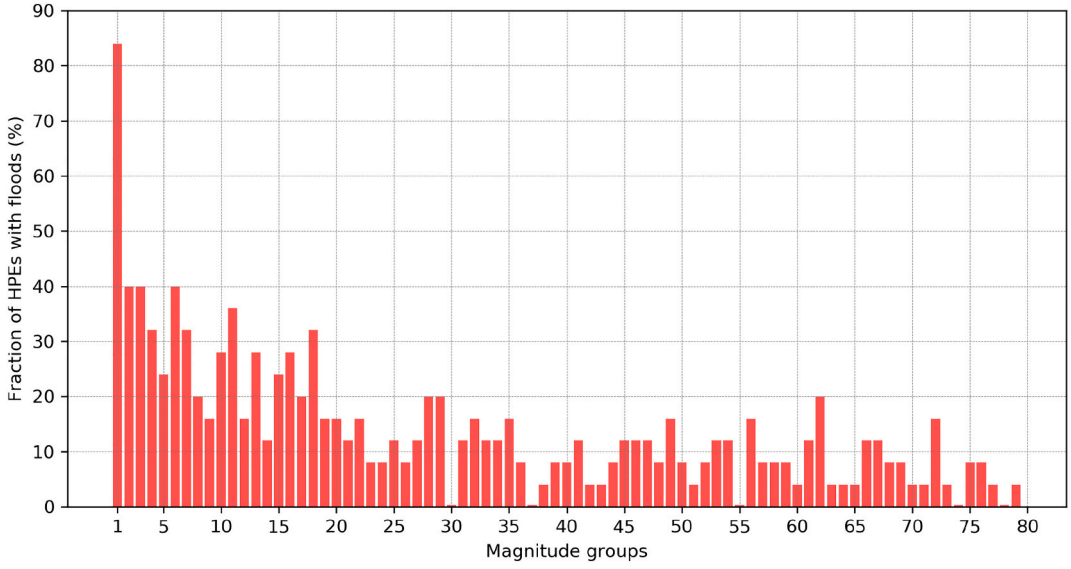

Fig. 6. Relationship between the magnitude of events and flood occurrence. Each magnitude bin is made of 25 events. The magnitude of the bins decreases in the x-axis from left to right, so that bin 1 is composed of the 25 most hazardous cases. The fraction of HPEs with floods indicates (in percent) how many of the events in each bin caused severe flooding.

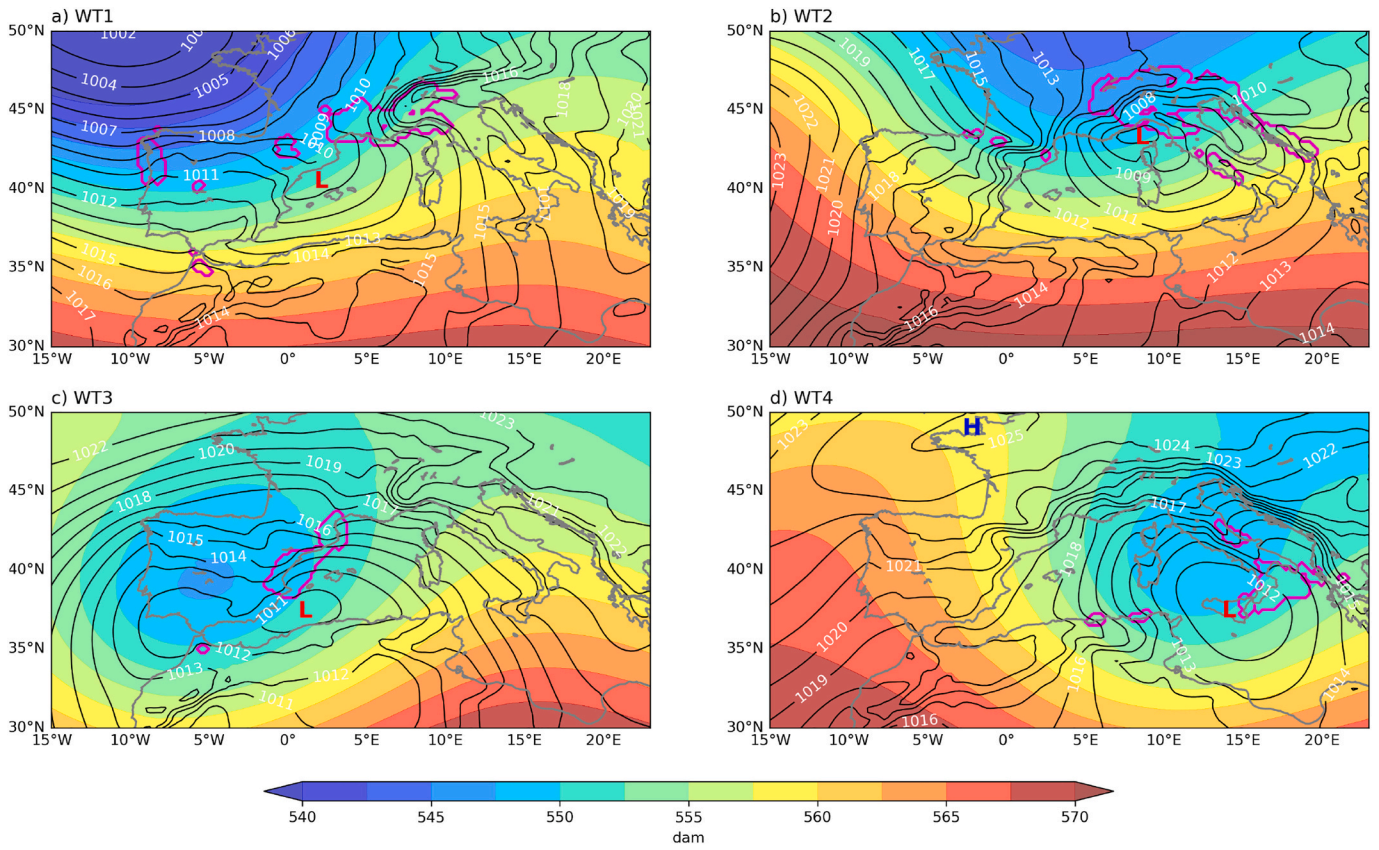

Fig. 7. Mean sea level pressure (black contours, hPa), geopotential height (colours, dam) and daily precipitation (magenta contour, amounts above 10 mm) of the four most frequent atmospheric patterns associated with hazardous precipitation in the western Mediterranean region, referred to as weather type 1 (a), 2 (b), 3 (c) and 4 (d).

explained a higher fraction of the variance; however, we think that working with a reduced number of weather types is much more practical and enlightening. As stated above, here weather types are based on two classic atmospheric variables; sea level pressure and 500 hPa geopotential height, represented in Fig. 7 by black contours and colour shades respectively. In addition, we have introduced daily precipitation in the weather type classification, so that we can also identify the areas most exposed to rainfall, marked with a magenta contour in Fig. 7.

These four predominant atmospheric patterns are well recognizable and agree well with the spatial distribution of the frequency of hazardous rains shown in Fig. 5. Weather type 1 (Fig. 7a) is characterized by a low-pressure area in the Atlantic, both at low and high levels. In this case, an upper-level ridge could emerge from the Mediterranean toward Central Europe generating a block pattern. Usually a secondary low pressure system forms off the coast of the Spanish Levant as a result of topographic troughing to the lee of the Iberian Peninsula, which helps to organize a warm and moist flow at low levels. Under this situation, the northern sector of the WMR, especially south-eastern France and north-western Italy, is usually the most impacted because it is very exposed to south-southeasterly winds. Weather type 2 (Fig. 7b) is marked by a Mediterranean cyclogenesis: a low-pressure system develops at the leading edge of a trough digging south into the Mediterranean Sea. The abrupt topography of the surrounding region is crucial in the generation of a low-level precursor for this type of cyclogenesis. The alpine orographic effect makes the low center most frequently appear in the Gulf of Genoa (Genoa Low), as reflected in Fig. 7b. The heavy rainfall generated by this type of cyclone especially affects the Alps and the areas by the Ligurian Sea, although intense precipitation could also occur in other parts of Italy, such as on the coasts of the Tuscany and Lazio regions. Weather type 3 (Fig. 7c) is well known in Spain: an upper level cut-off low, originated from an Atlantic trough, is situated in the vicinity of the Iberian Peninsula. Simultaneously, an extensive low-pressure zone at lower levels emerges from North Africa giving rise to an intense easterly flow along the Levant coast. Torrential rains usually appear in this Spanish coastal region when this synoptic pattern is present. The French region of Languedoc-Roussillon could also be affected by this weather type, especially its southern part. Finally, Weather type 4 (Fig. 7d) is especially hazardous for southern Italy. An upper level trough dives south from Central Europe with its axis tilted to the west and, at the surface, a low-pressure system develops and moves northward from Africa, just like for type 3, but in this case located further east. Calabria and Sicily are the most affected in this case because they are positioned at the leading edge of the trough, where the strongest dynamic forcings tend to occur. The south-eastern coast of these territories is particularly exposed because it receives directly the warm and humid winds from the Ionian Sea. In addition, some areas facing the Adriatic Sea, such as the Abruzzo region, may also record heavy rains under this situation.

But, which of these four meteorological situations is the most frequent? The answer to this question is found in Fig. 8a, showing the percentage of events associated with each atmospheric pattern. The weather type causing most episodes is number 2, with 31.1%, followed by 1, 4 and 3, in this order. Almost 5% of the episodes are undefined cases, not associated with any of the four atmospheric patterns considered. Since the detected episodes have been ordered according to their magnitude, we can also analyse the synoptic configurations leading to the most extraordinary events. Fig. 8b is identical to Fig. 8a but, instead of taking into account all identified events, we now consider only the 100 cases with the greatest magnitude. 40% of the most severe cases are produced by weather type 1, so it is perhaps the most hazardous pattern. Type 2, although frequently causing HPEs, appears to have a low potential to produce extraordinary events, being responsible for around

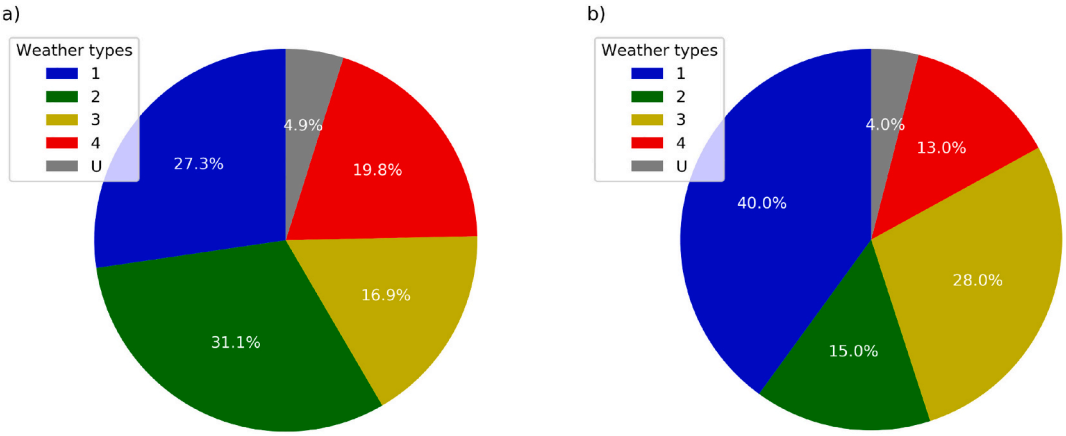

Fig. 8. Fraction of events (in %) associated with weather type 1 (blue), 2 (green), 3 (yellow) and 4 (red), for total episodes (a) and for the top 100 cases in the magnitude ranking (b). Gray indicates the fraction of undefined (U) events, not associated with any of the four types considered. (For interpretation of the references to color in this figure legend, the reader is referred to the web version of this article.)

15% of those. In contrast, weather type 3, despite being the least frequent, shows a greater capacity to produce exceptional cases, with a share of more than 25%. Conversely, type 4 is quite frequent, but it is the pattern associated with the least number of exceptional cases, only 13%. About 4% of the most extraordinary episodes have an undefined pattern, different from 1, 2, 3 and 4.

Different causes could explain why some weather types generate more extraordinary cases than others, which is a subject that is beyond the scope of this study. But one of the reasons that seems more evident from observing Fig. 7 is that the effective area exposed to maritime winds during a type 1 or 3 atmospheric pattern is greater than when there is a type 2 or 4. In addition, for weather types 1 and 3, the presence of an emerging blocking high to the east is also common, which could cause these situations to be more persistent.

4.4. Temporal distribution of hazardous rains

Fig. 9a shows a bar diagram with the average percentage of total annual events occurring monthly, indicating with different colours for each bar, the fractions corresponding to each of the four recurrent weather types discussed previously. Most episodes take place in autumn (confirming previous knowledge, e.g. Font, 1983; Llasat et al., 2013b), with almost half of all those registered each year concentrated in this season. The incidence of HPEs in either September, October or November is close to 15% of the annual total, with December and January being also relatively prone to hazardous rainfall. In contrast, during the rest of the year from February to August, only about 5% of events per month occur. Contributions to winter months are more usual in the eastern part of the WMR, that is to say, Italy and, specifically, the South of Italy. As an example, in region 6 more than 25% of total cases occur in December and January (not shown).

In general, weather type 1 is predominant for the cases occurring in the months with most events (September, October, November and December). However, for most of the warm season, from May to August, other atmospheric patterns cause more events, especially type 2. This is largely due to the Azores subtropical high moving poleward and displacing Atlantic low-pressure systems further north during summer, therefore preventing them from directly affecting the WMR. For this same reason, during the warmest months (July and August) there are almost no events associated with weather type 3. In the first part of the year, from January to April, the four types cause practically the same number of cases.

Finally, if we only consider the most severe cases, the top 100 episodes in our magnitude ranking, the seasonality is much more

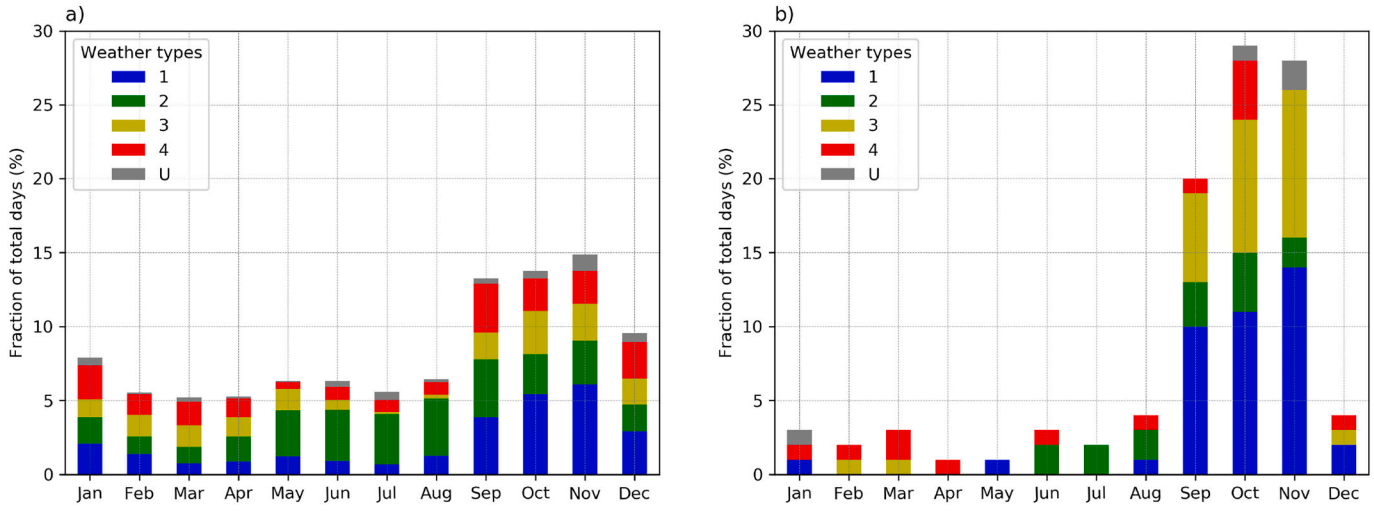

Fig. 9. Temporal distribution of potentially catastrophic rainfall in the western Mediterranean region, for total episodes (a) and for the 100 most hazardous cases (b). Bars indicate the percentage of events (on average) that occur each month. Gray indicates the fraction of undefined (U) events, not associated with any of the four types considered.

pronounced (Fig. 9b), that is to say, practically all the extraordinary episodes take place in the autumn months. During September, October and November in conjunction, more than 75% of all yearly episodes are recorded. This indicates that cases occurring during the rest of the year are usually minor episodes. Some of these minor cases could occasionally cause major damage if the rains are concentrated in a vulnerable place, but only very rarely will there be events that severely affect a vast region. The extraordinary autumn events are mainly caused by weather type 1, with type 3 being also very relevant, which is congruent with results in Fig. 8b.

4.5. Final dataset and examples

To conclude, we collect all the presented information into a file in CSV (comma-separated values) format, which is available for download in the Supplementary Material section. The file contains data from the 1991 daily episodes detected. Information in the HPEs database is organized in columns and each row corresponds to a single event. As an example, Table 1 shows the data for the first 25 events. Because in the database the episodes are positioned according to their magnitude (first column), these are the 25 most extraordinary cases recorded in the whole period. Columns 2 and 3 in Table 1 show, respectively, each episode's date and affected regions. If an event affects more than one region, they will be linked by a hyphen (e.g. "R1-R2", if the event affects regions 1 and 2). Column 4 shows the weather type associated with each daily event and column 5 indicates whether or not there was flooding according to FLOODHYMEX and EM-DAT data. In addition, four additional columns can be found in the CSV file, showing, for each episode, the total area affected and gridded precipitation characteristics (maximum, mean and standard deviation).

Finally, we show four representative examples of HPEs occurred in the 1980s in different areas of the WMR and in different months, one case for each of the four weather types described before, all of which caused severe flooding (please, find them in the top 100 of our ranking). Fig. 10 depicts sea level pressure and 500 hPa geopotential height (from ERA5) at 12 UTC for the day of the event and Fig. 11 total accumulated precipitation (from MESCAN) for the four daily episodes. The first of these corresponds to the case of 7 November 1982, which is the first episode in our ranking. The synoptic situation that produced the event (Fig. 10a) clearly corresponds to this weather type, with a deep cyclone over the Atlantic, blocked by an anticyclonic ridge to the east. The persistent southerly winds, which transported large amounts of moisture from the Atlantic (Insua-Costa et al., 2019), left the most notable precipitation records (Fig. 11a) in the Pyrenees and in the south-eastern sector of the French Massif Central (region 2). The weather type 2 example occurred during 23 August 1984. Heavy rainfall was caused by a low-pressure system generated on the leading edge of a pronounced trough entering the Mediterranean from the northwest. Therefore, although the surface low formed slightly to the west of the Gulf of Genoa in this case (Fig. 10b), it corresponds to a weather type 2. This episode especially affected regions 3 and 4, causing catastrophic floods in northern Italy, although heavy rainfall also impacted region 6 (Fig. 11b) and floods extended to Belgium and Spain. In Fig. 10c and 11c we show the meteorological configuration leading to the infamous flooding case of Tous (Spain), which is an example of weather type 3. The excessive rains recorded during 20 October 1982 in the Valencian Community (Fig. 11c) were in this case caused by a low pressure system over northern Africa, with a characteristic cut-off low aloft and intense southeasterly winds at lower levels (Fig. 10c). The fourth and last example took place on 17 April 1987 and was associated with low pressures in the east part of the WMR (Fig. 10d), clearly coinciding with weather type 4. In this case, heavy rains and floods affected southern Italy (Fig. 11d), where the low pressures were centred. All of these events are clear examples of the four most common atmospheric patterns found, although

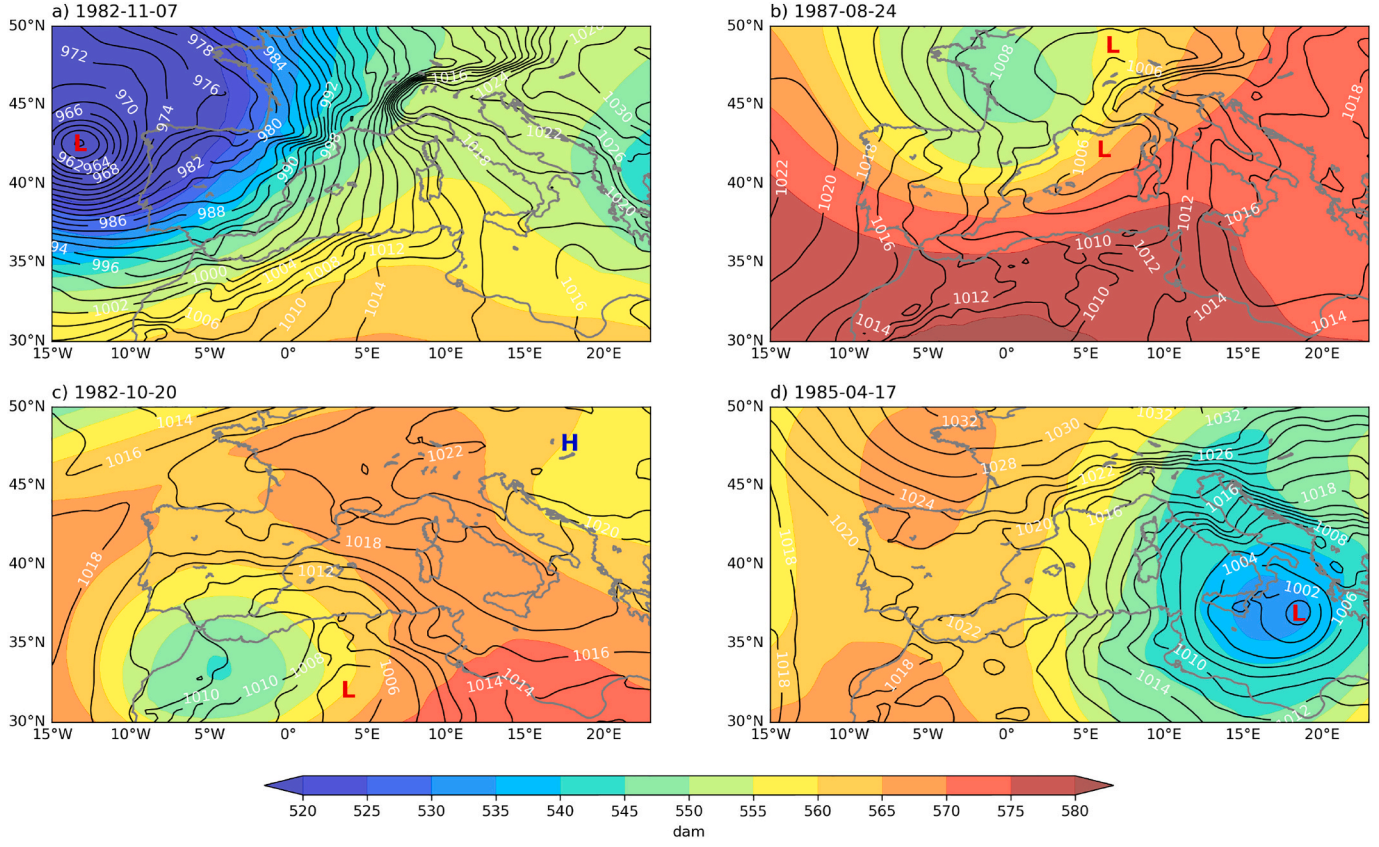

Fig. 10. Mean sea level pressure (contours, hPa) and 500 hPa geopotential height (colours, dam) for the example episodes of weather type 1 (a), 2 (b), 3 (c) and 4 (d). The fields are shown at 12 UTC on the day of the events.

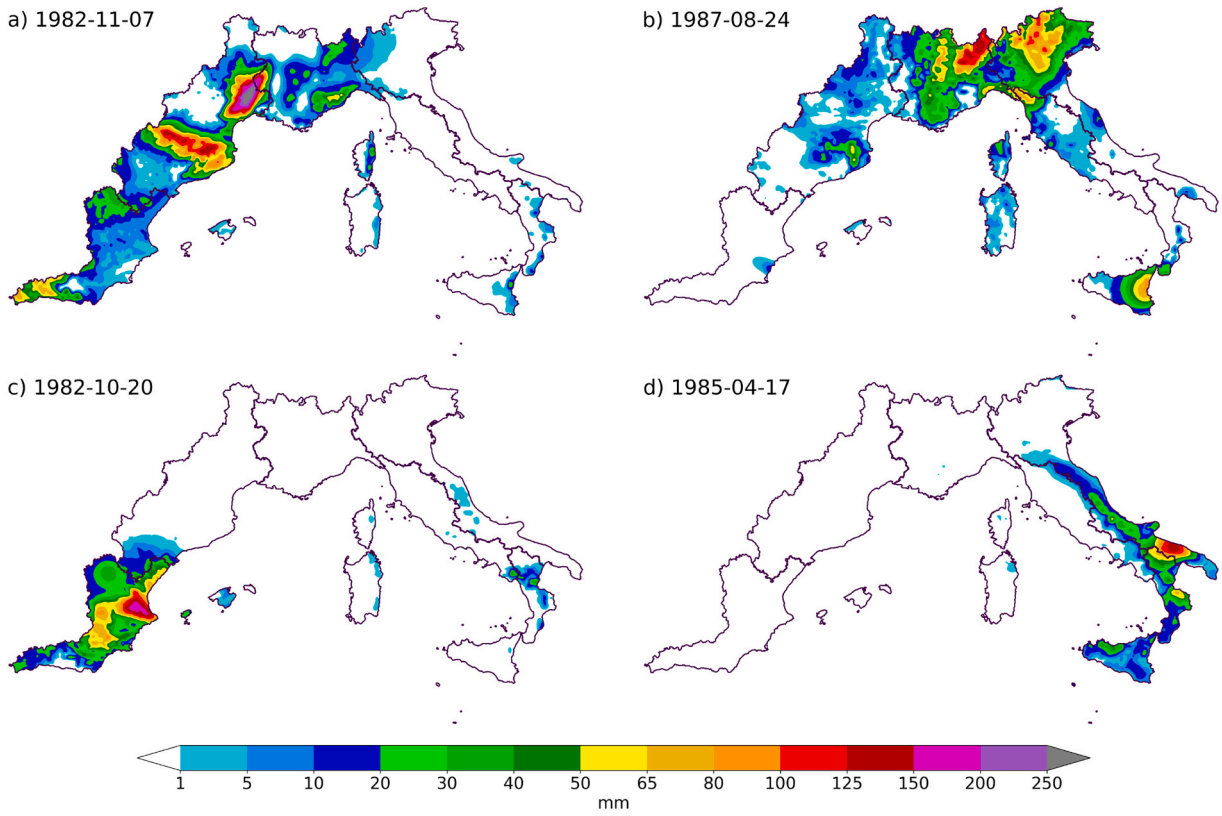

Fig. 11. Accumulated precipitation during the example episodes of Fig. 10.

in other cases the match between synoptic configuration and weather type is not so apparent. It is obvious that only four weather types cannot perfectly describe all situations and that there are events that do not exactly fit into any of them, especially summer cases, when the synoptic scale forcings are generally less important.

5. Summary and conclusions

The main objective of this work was to build a database, condensing and unifying the information on all potentially catastrophic precipitation episodes occurring in the western Mediterranean region from 1980 to 2015. The events' detection was based on the MESCAN precipitation analysis system, a daily gridded high-resolution (5.5 km) dataset constructed from a combination of a downscaled reanalysis and interpolated rain gauge measurements. The procedure consisted in defining hazardous precipitation days by means of a spatially variable precipitation threshold. This threshold was constructed from the combination of a fixed threshold of 60 mm with a statistical one, based on the normalized daily precipitation anomaly. The procedure, which is similar to that in Liu et al. (2020) for defining an impact-related threshold, ensures that, for every point, precipitation on the detected dates is extreme as well as a truly high amount. Subsequently, we classified the detected potentially catastrophic days according to the atmospheric pattern present by using a principal component analysis approach. Finally, we ranked events by magnitude, which was defined using the excess rainfall above the threshold, as well as the total area affected. In order to validate the used methodology, we crossed our list of identified hazardous days with the FLOODHYMEX and EM-DAT flooding databases.

We summarize our main findings in the following ten conclusions:

C1. The total number of hazardous rainfall days detected across the entire Western Mediterranean in the 36-year period 1980–2015 is 1991. For each individual sub-region, this means that there are between 5 and 15 days per year, confirming the high frequency of occurrence of these type of episodes in the area.

C2. In the Western Mediterranean, most HPEs are concentrated in just three distinct coastal areas: the entire coastal stretch from Murcia (Spain) to Genoa (Italy), the east coast of Corsica and Sardinia and the Ionian coast of Calabria and Sicily.

C3. Hazardous rain episodes extend inland mainly through the Rhone Valley, as well as along the south east sectors of the French Massif Central and the Alps mountainous systems. The remaining events are unevenly distributed in different parts of the region.

C4. In addition to the proximity to the coast, the orientation of the latter is also crucial; in coastal areas facing south or east, frequent torrential rains are almost assured. In some places, this results in a well-defined border between recurrently affected and unaffected zones, such as in the Spanish Levant.

C5. Population density in the region is highest in coastal areas, precisely where potentially catastrophic precipitation is more frequent, which increases significantly flood risk. In particular, populations in the Valencian Community and in the Languedoc-Roussillon region are the ones exposed to a greater number of HPEs. In these coastal territories we found peaks of 30 events, almost 1 per year.

C6. The most favourable months for the development of dangerous rainfall situations are September, October and November, in which 40% of the cases recorded each year are concentrated (almost 15% in each of them).

C7. Major episodes (of greater magnitude) present a strict seasonality; the vast majority, more than 75%, are concentrated in the three autumn months (SON). From December to September HPEs can occur, but the atmosphere does not show a high potential to produce extraordinary amounts of rain. Therefore, episodes taking place in winter, spring or summer are generally less severe, although they can occasionally cause significant damage if their associated heavy rains are concentrated in a vulnerable location.

C8. The synoptic scale configurations leading to hazardous rainfall in the western Mediterranean are recurrent: only four weather types

explain most of the daily episodes.

C9. The synoptic configuration most frequently producing extraordinary (high magnitude) events is the following: a low-pressure system vertically extended to all tropospheric levels in the eastern Atlantic, forming a block pattern with an anticyclonic ridge located further east. This atmospheric pattern causes more than 40% of the major episodes.

C10. A block pattern such as the one described in the previous paragraph was the precursor of fatal episodes at the top of our ranking such as Piedmont 1994 or Gard 2002, demonstrating the potential of this atmospheric configuration for producing catastrophic damage.

In summary, our results shed light on different aspects of potentially catastrophic rains in the western Mediterranean. All information generated will be made public and available to other researchers, with the main objective of further expanding and improving the current knowledge on these catastrophic weather events. In future work we will adapt episode detection for the using of the new European CERRA reanalysis (in process; https://climate.copernicus.eu/copernicus-regional-reanalysis-europe-cerra), which will replace MESCAN introducing major improvements. The CERRA system will provide precipitation data in near-real time, allowing us to update the hazardous rainfall database with that same frequency.

Declaration of Competing Interest

The authors declare that they have no conflict of interest.

Acknowledgements

Funding comes from the Spanish Ministerio de Economia y Competitividad OPERMO (CGL2017-89859-R to GMM and DIC), CLICES (CGL2017-83866-C3-2-R to MLC) and M-CostAdapt (CTM2017-83655-C2-2-R to MCLL) projects, the European Union Interreg V POCTEFA project (EFA210/16 PIRAGUA to MCLL) and the CRETUS strategic partnership (AGRUP2015/02 to GMM and DIC). All these programs are co-funded by the European Union ERDF. DIC and MLC were awarded a pre-doctoral FPI (PRE2018-084425) and FPU (FPU2017/02166) grant, respectively, both from the Spanish Ministry of Science, Innovation and Universities. Computation took place at CESGA (Centro de Supercomputacion de Galicia), Santiago de Compostela, Galicia, Spain.

Author statement

DIC performed the data analysis, created the figures and wrote the first manuscript draft. MLC was in charge of carrying out the weather type classification. GMM and MCLL contributed with ideas, interpretation of the results, and manuscript revisions. The initial concept of the paper as well as the design of the experiment was a joint work of all the authors.

Appendix A. Supplementary data

Supplementary data to this article can be found online at https://doi.org/10.1016/j.atmosres.2021.105521.

References

Adhikari, P., Hong, Y., Douglas, K.R., Kirschbaum, D.B., Gourley, J., Adler, R., Brakenridge, G.R., 2010. A digitized global flood inventory (1998-2008): Compilation and preliminary results. Nat. Hazards. https://doi.org/10.1007/s11069-010-9537-2.

Alpert, P., Ben-Gai, T., Baharad, A., Benjamini, Y., Yekutieli, D., Colacino, M., Diodato, L., Ramis, C., Homar, V., Romero, R., Michaelides, S., Manes, A., 2002. The paradoxical increase of Mediterranean extreme daily rainfall in spite of decrease in total values. Geophys. Res. Lett. https://doi.org/10.1029/2001GL013554.

Barredo, J.I., 2007. Major flood disasters in Europe: 1950-2005. Nat. Hazards 42, 125–148. https://doi.org/10.1007/s11069-006-9065-2.

Barriendos, M., Coeur, D., Lang, M., Llasat, M.C., Naulet, R., Lemaitre, F., Barrera, A., 2003. Stationarity analysis of historical flood series in France and Spain (14th–20th centuries). Nat. Hazards Earth Syst. Sci. https://doi.org/10.5194/nhess-3-583-2003.

Belo-Pereira, M., Dutra, E., Viterbo, P., 2011. Evaluation of global precipitation data sets over the Iberian Peninsula. J. Geophys. Res.-Atmos. https://doi.org/10.1029/2010JD015481.

Brooks, H.E., Stensrud, D.J., 2000. Climatology of heavy rain events in the United States from hourly precipitation observations. Mon. Weather Rev. https://doi.org/10.1175/1520-0493(2000)128<1194:COHREI>2.0.CO;2.

Brunetti, M., Maugeri, M., Nanni, T., Navarra, A., 2002. Droughts and extreme events in regional daily Italian precipitation series. Int. J. Climatol. https://doi.org/10.1002/joc.751.

Buzzi, A., Tartaglione, N., Malguzzi, P., 1998. Numerical simulations of the 1994 Piedmont flood: role of orography and moist processes. Mon. Weather Rev. 126, 2369–2383. https://doi.org/10.1175/1520-0493(1998)126<2369:NSOTPF>2.0.CO;2.

Cattell, R.B., 1966. The scree test for the number of factors. Multivar. Behav. Res. https://doi.org/10.1207/s15327906mbr0102_10.

Cornes, R.C., van der Schrier, G., van den Besselaar, E.J., Jones, P.D., 2018. An ensemble version of the E-OBS temperature and precipitation data sets. J. Geophys. Res.-Atmos. https://doi.org/10.1029/2017JD028200.

Diakakis, M., 2014. An inventory of flood events in Athens, Greece, during the last 130 years. Seasonality and spatial distribution. J. Flood Risk Manag. https://doi.org/10.1111/jfr3.12053.

Donat, M.G., Lowry, A.L., Alexander, L.V., O'Gorman, P.A., Maher, N., 2016. Addendum: more extreme precipitation in the world's dry and wet regions. Nat. Clim. Chang. https://doi.org/10.1038/nclimate3160.

Drobinski, P., Ducrocq, V., Alpert, P., Anagnostou, E., Béranger, K., Borga, M., Braud, I., Chanzy, A., Davolio, S., Delrieu, G., Estournel, C., Filali Boubrahmi, N., Font, J., Grubišić, V., Gualdi, S., Homar, V., Ivančan-Picek, B., Kottmeier, C., Kotroni, V., Lagouvardos, K., Lionello, P., Llasat, M.C., Ludwig, W., Lutoff, C., Mariotti, A., Richard, E., Romero, R., Rotunno, R., Roussot, O., Ruin, I., Somot, S., Taupier-Letage, I., Tintor, J., Uijlenhoet, R., Wernli, H., 2014. HYMEX: A 10-year multidisciplinary program on the mediterranean water cycle. Bull. Am. Meteorol. Soc. 95, 1063–1082. https://doi.org/10.1175/BAMS-D-12-00242.1.

Ducrocq, V., Braud, I., Davolio, S., Ferretti, R., Flamant, C., Jansa, A., Kalthoff, N., Richard, E., Taupier-Letage, I., Ayral, P.A., Belamari, S., Berne, A., Borga, M., Boudevillain, B., Bock, O., Boichard, J.L., Bouin, M.N., Bousquet, O., Bouvier, C., Chiggiato, J., Cimini, D., Corsmeier, U., Coppola, L., Cocquerez, P., Defer, E., Delanoë, J., Di Girolamo, P., Doerenbecher, A., Drobinski, P., Dufournet, Y., Fourrié, N., Gourley, J.J., Labatut, L., Lambert, D., Le Coz, J., Marzano, F.S., Molinié, G., Montani, A., Nord, G., Nuret, M., Ramage, K., Rison, W., Roussot, O., Said, F., Schwarzenboeck, A., Testor, P., Van Baelen, J., Vincendon, B., Aran, M., Tamayo, J., 2014. HyMeX-SOP1: The field campaign dedicated to heavy precipitation and flash flooding in the northwestern mediterranean. Bull. Am. Meteorol. Soc. https://doi.org/10.1175/BAMS-D-12-00244.1.

Easterling, D.R., Meehl, G.A., Parmesan, C., Changnon, S.A., Karl, T.R., Mearns, L.O., 2000. Climate Extremes: Observations, Modeling, and Impacts. https://doi.org/10.1126/science.289.5487.2068.

Esteban, P., Jones, P.D., Martín-Vide, J., Mases, M., 2005. Atmospheric circulation patterns related to heavy snowfall days in Andorra, Pyrenees. Int. J. Climatol. https://doi.org/10.1002/joc.1103.

Federico, S., Avolio, E., Pasqualoni, L., Bellecci, C., 2008. Atmospheric patterns for heavy rain events in Calabria. Nat. Hazards Earth Syst. Sci. https://doi.org/10.5194/nhess-8-1173-2008.

Fiori, E., Comellas, A., Molini, L., Rebora, N., Siccardi, F., Gochis, D.J., Tanelli, S., Parodi, A., 2014. Analysis and hindcast simulations of an extreme rainfall event in the Mediterranean area: The Genoa 2011 case. Atmos. Res. https://doi.org/10.1016/j.atmosres.2013.10.007.

Font, I., 1983. Climatologia de España y Portugal (in Spanish).

Gao, X., Pal, J.S., Giorgi, F., 2006. Projected changes in mean and extreme precipitation over the Mediterranean region from a high resolution double nested RCM simulation. Geophys. Res. Lett. https://doi.org/10.1029/2005GL024954.

Gaume, E., Borga, M., Llasat, M.C., Maouche, S., Lang, M., Diakakis, M., 2016. Mediterranean extreme floods and flash floods. In: Editions, I. (Ed.), The Mediterranean Region under Climate Change, A Scientific Update. Marseille. Chapter 3, pp. 133–144.

Gilabert, J., Llasat, M.C., 2018. Circulation weather types associated with extreme flood events in Northwestern Mediterranean. Int. J. Climatol. https://doi.org/10.1002/joc.5301.

Goubanova, K., Li, L., 2007. Extremes in temperature and precipitation around the Mediterranean basin in an ensemble of future climate scenario simulations. Glob. Planet. Chang. https://doi.org/10.1016/j.gloplacha.2006.11.012.

Häggmark, L., Ivarsson, K.I., Gollvik, S., Olofsson, P.O., 2000. Mesan, an operational mesoscale analysis system. Tellus Ser. A Dyn. Meteorol. Oceanogr. https://doi.org/10.3402/tellusa.v52i1.12250.

Herrera, S., Gutiérrez, J.M., Ancell, R., Pons, M.R., Frías, M.D., Fernández, J., 2012. Development and analysis of a 50-year high-resolution daily gridded precipitation dataset over Spain (Spain02). Int. J. Climatol. https://doi.org/10.1002/joc.2256.

Hersbach, H., Dee, D., 2016. ERA5 Reanalysis is in Production. URL. http://www.ecmwf.int/sites/default/files/elibrary/%0A2016/16299-newsletter-no147-spring-2016.pdf.

Houssos, E.E., Lolis, C.J., Bartzokas, A., 2008. Atmospheric circulation patterns associated with extreme precipitation amounts in Greece. Adv. Geosci. https://doi.org/10.5194/adgeo-17-5-2008.

Insua-Costa, D., Miguez-Macho, G., Llasat, C., 2019. Local and remote moisture sources for extreme precipitation: A study of the two catastrophic 1982 western Mediterranean episodes. Hydrol. Earth Syst. Sci. https://doi.org/10.5194/hess-23-3885-2019.

Isotta, F.A., Frei, C., Weilguni, V., Perčec Tadić, M., Lassègues, P., Rudolf, B., Pavan, V., Cacciamani, C., Antolini, G., Ratto, S.M., Munari, M., Micheletti, S., Bonati, V., Lussana, C., Ronchi, C., Panettieri, E., Marigo, G., Vertačnik, G., 2014. The climate of daily precipitation in the Alps: Development and analysis of a high-resolution grid dataset from pan-Alpine rain-gauge data. Int. J. Climatol. https://doi.org/10.1002/joc.3794.

Jansa, A., Alpert, P., Arbogast, P., Buzzi, A., Ivancan-Picek, B., Kotroni, V., Llasat, M.C., Ramis, C., Richard, E., Romero, R., Speranza, A., 2014. MEDEX: A general overview. https://doi.org/10.5194/nhess-14-1965-2014.

Jansa, A., Genoves, A., Picornell, M.A., Campins, J., Riosalido, R., Carretero, O., 2001. Western Mediterranean cyclones and heavy rain. Part 2: Statistical approach. Meteorol. Appl. 8, 43–56.

Lana, A., Campins, J., Genovés, A., Jansà, A., 2007. Atmospheric patterns for heavy rain events in the Balearic Islands. Adv. Geosci. https://doi.org/10.5194/adgeo-12-27-2007.

Lemus-Canovas, M., Lopez-Bustins, J.A., Martin-Vide, J., Royé, D., 2019a. synoptReg: An R package for computing a synoptic climate classification and a spatial regionalization of environmental data. Environ. Model. Softw. https://doi.org/10.1016/j.envsoft.2019.04.006.

Lemus-Canovas, M., Lopez-Bustins, J.A., Trapero, L., Martin-Vide, J., 2019b. Combining circulation weather types and daily precipitation modelling to derive climatic precipitation regions in the Pyrenees. Atmos. Res. https://doi.org/10.1016/j.atmosres.2019.01.018.

Lemus-Canovas, M., Ninyerola, M., Lopez-Bustins, J.A., Manguan, S., Garcia-Sellés, C., 2019c. A mixed application of an objective synoptic classification and spatial regression models for deriving winter precipitation regimes in the Eastern Pyrenees. Int. J. Climatol. https://doi.org/10.1002/joc.5948.

Liu, W., Wu, J., Tang, R., Ye, M., Yang, J., 2020. Daily precipitation threshold for rainstorm and flood disaster in the mainland of China: An economic loss perspective. Sustainability (Switzerland) 12. https://doi.org/10.3390/SU12010407.

Llasat, C., Llasat-Botija, M., Petrucci, O., Pasqua, A.A., Rossello, J., Vinet, F., Boissier, L., 2013a. Floods in the north-western Mediterranean region: Presentation of the HYMEX database and comparison with pre-existing global databases. Houille Blanche. https://doi.org/10.1051/lhb/2013001.

Llasat, M.C., Llasat-Botija, M., Prat, M.A., Porcú, F., Price, C., Mugnai, A., Lagouvardos, K., Kotroni, V., Katsanos, D., Michaelides, S., Yair, Y., Savvidou, K., Nicolaides, K., 2010. High-impact floods and flash floods in Mediterranean countries: The FLASH preliminary database. Adv. Geosci. https://doi.org/10.5194/adgeo-23-47-2010.

Llasat, M.C., Llasat-Botija, M., Petrucci, O., Pasqua, A.A., Rosselló, J., Vinet, F., Boissier, L., 2013b. Towards a database on societal impact of Mediterranean floods within the framework of the HYMEX project. Nat. Hazards Earth Syst. Sci. https://doi.org/10.5194/nhess-13-1337-2013.

Llasat, M.C., Marcos, R., Turco, M., Gilabert, J., Llasat-Botija, M., 2016. Trends in flash flood events versus convective precipitation in the Mediterranean region: The case of Catalonia. J. Hydrol. https://doi.org/10.1016/j.jhydrol.2016.05.040.

Lopez-Bustins, J.A., Lemus-Canovas, M., 2020. The influence of the Western Mediterranean Oscillation upon the spatio-temporal variability of precipitation over Catalonia (northeastern of the Iberian Peninsula). Atmos. Res. https://doi.org/10.1016/j.atmosres.2019.104819.

Martínez, C., Campins, J., Jansà, A., Genovés, A., 2008. Heavy rain events in the Western Mediterranean: an atmospheric pattern classification. Adv. Sci. Res. https://doi.org/10.5194/asr-2-61-2008.

Martin-Vide, J., Lopez-Bustins, J.A., 2006. The Western Mediterranean Oscillation and rainfall in the Iberian Peninsula. Int. J. Climatol. https://doi.org/10.1002/joc.1388.

Martin-Vide, J., Sanchez-Lorenzo, A., Lopez-Bustins, J.A., Cordobilla, M.J., Garcia-Manuel, A., Raso, J.M., 2008. Torrential rainfall in northeast of the Iberian Peninsula: synoptic patterns and WeMO influence. Adv. Sci. Res. https://doi.org/10.5194/asr-2-99-2008.

McPhillips, L.E., Chang, H., Chester, M.V., Depietri, Y., Friedman, E., Grimm, N.B., Kominoski, J.S., McPhearson, T., Méndez-Lázaro, P., Rosi, E.J., Shafiei Shiva, J., 2018. Defining Extreme Events: A Cross-Disciplinary Review. Earth's Future 6, 441–455. https://doi.org/10.1002/2017EF000686.

Milelli, M., Llasat, M.C., Ducrocq, V., 2006. The cases of June 2000, November 2002 and September 2002 as examples of mediterranean floods. Nat. Hazards Earth Syst. Sci. https://doi.org/10.5194/nhess-6-271-2006.

Min, S.K., Zhang, X., Zwiers, F.W., Hegerl, G.C., 2011. Human contribution to more-intense precipitation extremes. Nature. https://doi.org/10.1038/nature09763.

Philipp, A., Beck, C., Huth, R., Jacobeit, J., 2016. Development and comparison of circulation type classifications using the COST 733 dataset and software. Int. J. Climatol. https://doi.org/10.1002/joc.3920.

Ramos, A.M., Trigo, R.M., Liberato, M.L., 2014. A ranking of high-resolution daily precipitation extreme events for the Iberian Peninsula. Atmos. Sci. Lett. https://doi.org/10.1002/asl2.507.

Ricard, D., Ducrocq, V., Auger, L., 2012. A climatology of the mesoscale environment associated with heavily precipitating events over a northwestern Mediterranean area. J. Appl. Meteorol. Climatol. https://doi.org/10.1175/JAMC-D-11-017.1.

Richman, M.B., 1986. Rotation of Principal Components. https://doi.org/10.1002/joc.3370060305.

Romero, R., Guijarro, J., Ramis, C., Alonso, S., 1998. A 30-year (1964–1993) daily rainfall data base for the Spanish Mediterranean regions: first exploratory study. Int. J. Climatol. https://doi.org/10.1002/(sici)1097-0088(199804)18:5<541::aid-joc270>3.3.co;2-e.

Romero, R., Sumner, G., Ramis, C., Genovés, A., 1999. A classification of the atmospheric circulation patterns producing significant daily rainfall in the Spanish Mediterranean area. Int. J. Climatol. https://doi.org/10.1002/(SICI)1097-0088(19990615)19:7<765::AID-JOC388>3.0.CO;2-T.

Romero, R., Doswell, C.A., Ramis, C., Romero III, R., C.A.D, Ramis, C., 2000. Mesoscale numerical study of two cases of long-lived quasi-stationary convective systems over Eastern Spain. Mon. Weather Rev. 128, 3731–3751. https://doi.org/10.1175/1520-0493(2001)129<3731:MNSOTC>2.0.CO;2.

Sánchez, E., Gallardo, C., Gaertner, M.A., Arribas, A., Castro, M., 2004. Future climate extreme events in the Mediterranean simulated by a regional climate model: A first approach. Glob. Planet. Chang. https://doi.org/10.1016/j.gloplacha.2004.06.010.

Schär, C., Ban, N., Fischer, E.M., Rajczak, J., Schmidli, J., Frei, C., Giorgi, F., Karl, T.R., Kendon, E.J., Tank, A.M., O'Gorman, P.A., Sillmann, J., Zhang, X., Zwiers, F.W., 2016. Percentile indices for assessing changes in heavy precipitation events. Clim. Chang. 137, 201–216. https://doi.org/10.1007/s10584-016-1669-2.

Seneviratne, S.I., Nicholls, N., Easterling, D., Goodess, C.M., Kanae, S., Kossin, J., Luo, Y., Marengo, J., Mc Innes, K., Rahimi, M., Reichstein, M., Sorteberg, A., Vera, C., Zhang, X., Rusticucci, M., Semenov, V., Alexander, L.V., Allen, S., Benito, G., Cavazos, T., Clague, J., Conway, D., Della-Marta, P.M., Gerber, M., Gong, S., Goswami, B.N., Hemer, M., Huggel, C., Van den Hurk, B., Kharin, V.V., Kitoh, A., Klein Tank, A.M., Li, G., Mason, S., Mc Guire, W., Van Oldenborgh, G.J., Orlowsky, B., Smith, S., Thiaw, W., Velegrakis, A., Yiou, P., Zhang, T., Zhou, T., Zwiers, F.W., 2012. Changes in Climate Extremes and Their Impacts on the Natural Physical Environment. volume 9781107025. https://doi.org/10.1017/CBO9781139177245.006.

Serrano-Notivoli, R., Beguería, S., Saz, M.Á., Longares, L.A., De Luis, M., 2017. SPREAD: A high-resolution daily gridded precipitation dataset for Spain - an extreme events frequency and intensity overview. Earth Syst. Sci. Data. https://doi.org/10.5194/essd-9-721-2017.

Soci, C., Bazile, E., Besson, F.O., Landelius, T., 2016. High-resolution precipitation re-analysis system for climatological purposes. Tellus Ser. A Dyn. Meteorol. Oceanogr. 68 https://doi.org/10.3402/tellusa.v68.29879.

Taillefer, F., 2002. CANARI Technical Documentation based on ARPEGE cycle CY25T1 (AL25T1 for ALADIN).

Tramblay, Y., Somot, S., 2018. Future evolution of extreme precipitation in the Mediterranean. Clim. Chang. https://doi.org/10.1007/s10584-018-2300-5.

Trapero, L., Bech, J., Duffourg, F., Esteban, P., Lorente, J., 2013. Mesoscale numerical analysis of the historical November 1982 heavy precipitation event over Andorra (Eastern Pyrenees). Nat. Hazards Earth Syst. Sci. 13, 2969–2990. https://doi.org/10.5194/nhess-13-2969-2013.